molecular pharmaceutics

Article

pubs.acs.org/molecularpharmaceutics

In Vivo Optical Imaging of Membrane-Type Matrix Metalloproteinase (MT-MMP) Activity

Lei Zhu,[†,‡] Fan Zhang,[†] Ying Ma,[†] Gang Liu,[†] Kwangmeyung Kim,[§] Xuexun Fang,[‡] Seulki Lee,*[,†] and Xiaoyuan Chen*[,†]

[†]Laboratory of Molecular Imaging and Nanomedicine (LOMIN), National Institute of Biomedical Imaging and Bioengineering (NIBIB), National Institutes of Health (NIH), Bethesda, Maryland 20892, United States

[‡]Key laboratory of Molecular Enzymology and Enzyme Engineering, Ministry of Education, Jilin University, Changchun 130023, P.R. China

[§]Biomedical Research Center, Korea Institute of Science and Technology, Seoul 136-791, Korea

Supporting Information

ABSTRACT: Herein we demonstrate for the first time that a fluorogenic probe can be used as an *in vivo* imaging agent for visualizing activities of membrane-tethered, membrane-type matrix metalloproteinases (MT-MMPs). An MT-MMP fluorogenic probe that consisted of an MT1-MMP (MMP-14) substrate and near-infrared (NIR) dye-quencher pair exhibited rapid, efficient boosts in fluorescence upon cleavage by MT1-MMP in tumor-bearing mice. In particular, unlike similar fluorogenic probes designed to target extracellular, soluble-type MMPs (EC-MMPs)—which can be cleared from the bloodstream after activation—the fluorescence signals activated by MT1-MMP enable clear visualization of MT1-MMP-positive tumors in animal models for up to 24 h. The results indicate that a simple form of a fluorogenic probe that is less effective in EC-MMP imaging is an effective probe for imaging MT-MMP activities *in vivo*. These findings can be widely applied to designing probes and to applications targeting various membrane-anchored proteases *in vivo*.

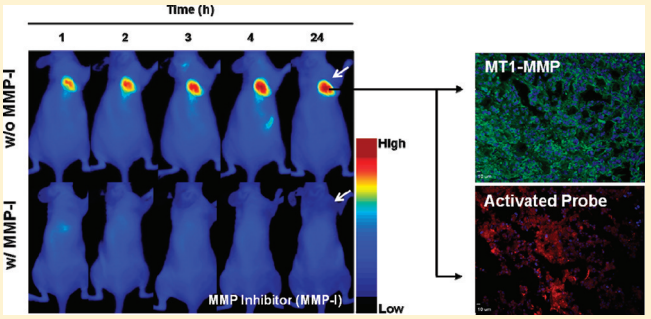

KEYWORDS: *activatable probe, fluorogenic probe, membrane-type matrix metalloproteinase, optical imaging, protease*

1. INTRODUCTION

Matrix metalloproteinases (MMPs) are a family of zinc-dependent endopeptidases and play a crucial role in various physiological processes, including extracellular matrix (ECM) remodeling, inflammatory processes, and in diseases such as cancer.[1−3] For example, MMPs are predominantly associated with tumorigenesis and control, and they regulate signaling pathways of angiogenesis and cancer cell growth and migration. MMPs have been well-documented to be related to cancer. To date, a total of 23 human MMPs have been characterized. Since deregulation of various MMPs is associated with multiple cancers, different types of MMPs have been important targets to understand MMP-related cancer mechanisms and treatment. In fact, a number of clinical trials using MMP inhibitors were started 20 years ago by several major pharmaceutical companies; however, the results of these trials turned out to be unsuccessful in phase III, since the trials failed to improve the survival rate of cancer patients.[4,5] After careful reevaluation of clinical studies, and based on the recent understanding of the role of MMPs in clinical cancer biology, it is now clear that the MMP function is more complex than originally thought, and the previous clinical studies were inappropriately designed.[3,6] Very recently, to improve understanding of the physiological roles of MMPs, a noninvasive, *in vivo* molecular imaging approach has been adopted, and its development has markedly advanced the utilization of MMP imaging probes.[7,8]

Noninvasive imaging of MMP proteolytic activity may provide valuable answers to fundamentally important biological questions, as well as information vital to drug development and clinical practice. For example, molecular imaging of MMP activity in animal models of tumors will help improve understanding of the physiological roles of MMPs in tumor microenvironments.[9] Since MMPs can be specific biomarkers, they can be used for early diagnosis and identification of tumors or to screen and monitor the efficacy of new anticancer therapeutic regimens by real-time imaging of MMP activities.[10] Recently, an MMP imaging probe has been applied to intraoperative, optical-imaging-guided surgery, which is an attractive new tool in the field of surgical oncology.[11]

Successful *in vivo* imaging of MMP activities largely depends on the utilization of MMP-specific molecular imaging probes.

Received: May 2, 2011
Revised: August 9, 2011
Accepted: October 20, 2011
Published: October 20, 2011

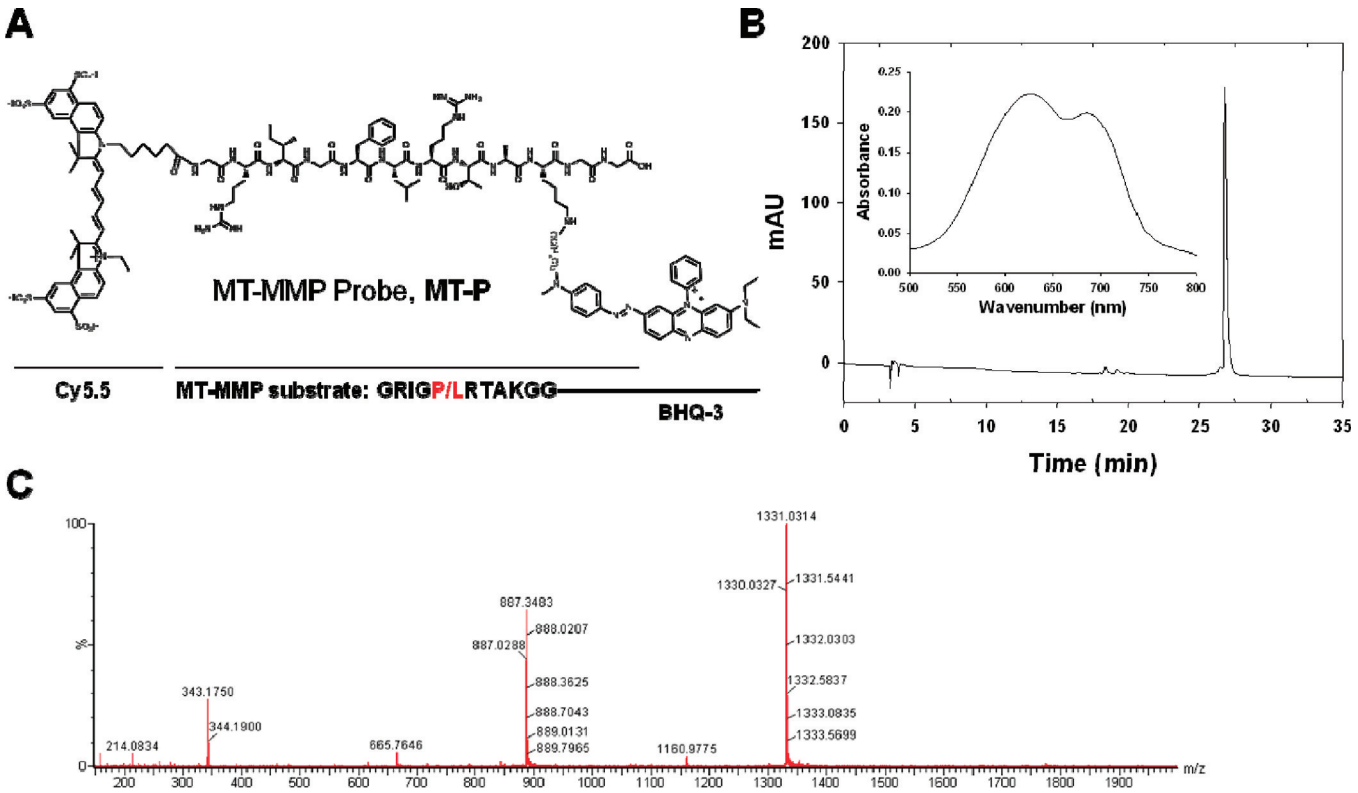

Figure 1. (A) Chemical structure of a MT-MMP-specific fluorogenic probe, MT-P. The cleavage site is between Phe and Leu. (B) HPLC and UV–vis (inset) spectra of MT-P. (C) LC/MS spectrum of MT-P.

To date, various kinds of MMP imaging probes have been developed for different imaging modalities and tested in animal models of disease. These probes have included fluorogenic substrate-based probes for optical imaging,[12,13] radiolabeled MMP inhibitors or antibodies for positron emission tomography (PET) and single photon emission computed tomography (SPECT),[14] and gadolinium-labeled MMP inhibitors for magnetic resonance imaging (MRI).[15] The most prominent imaging probes used for MMP imaging are fluorogenic, so-called molecular beacons or activatable probes.[16,17] The simplest form of fluorogenic probe consists of a near-infrared (NIR) fluorophore and a quencher conjugated to opposite ends of an MMP substrate. However, many of the reported fluorogenic probes have demonstrated limited *in vivo* applications, since the peptide substrates are often nonspecifically activated, providing high background signals, or are unstable and/or washed away in the bloodstream. To overcome these drawbacks, various types of MMP imaging probes have been reported that conjugate fluorogenic probes to linear poly(amino acids),[18] cell-penetrating peptides,[19] poly(ethylene glycols),[20] polymeric nanoparticles,[21] or dendrimers.[22] These probes have shown promising results *in vivo* with improved MMP-sensitivity; however, it should be pointed out that their target MMPs were mostly extracellular, soluble-type MMPs, such as MMP-2, -7, -9, and -13.

MMPs can be categorized into two types: secreted soluble-type (extracellular MMPs, EC-MMPs) and membrane-tethered type (membrane-type MMPs, MT-MMPs).[3] EC-MMPs are popular targets for *in vivo* imaging, because (i) their mechanisms are well-established, (ii) they are abundantly overexpressed in various tumors, and (iii) they are easily accessible, as they are located around the tumor tissues, compared to other overexpressing proteases on cellular membranes or in cells. Recent discoveries of MT-MMPs have been accompanied by descriptions of novel mechanisms of their roles in cancer biology, and MT-MMPs are the new focus of research to develop novel targets for MMP-related cancer therapy and imaging.[9,23] MT-MMPs are tethered to the plasma membrane via either a glycosylphosphatidyl inositol linkage or a transmembrane domain.[24] The physical location of MT-MMPs confers regulatory and functional mechanisms that are different than the EC-MMPs. Among the MT-MMPs, MT1-MMP (MMP-14) has been intensively studied because of its critical roles in EC-MMP activations, multiple signaling pathways, and tumor development.[3,25−28] For example; MT1-MMP activates EC-MMPs such as pro-MMP-2 and pro-MMP-13 and regulates their expression. In addition, MT1-MMP is also involved in the cleavage of cell surface receptors including tissue transglutaminase, CD44, pro-αv integrin, syndecan-1, low-density lipoprotein (LDL) receptor-related protein, and L-glycan. The expression of MT1-MMP is crucial for cancer cell growth in a 3D collagen-based matrix, suggesting that MT1-MMP has important roles not only in cancer invasion but also in overall tumor progression. Such unique features of MT1-MMP over typical EC-MMPs make it an interesting target as a biomarker and for tumor imaging. EC-MMPs have been extensively targeted for *in vivo* imaging; however, MT-MMP imaging has not been reported except for a few SPECT studies using a radiolabeled endogenous tissue inhibitor of MMP-2 (TIMP-2) in tumor-bearing mice and MT1-MMP antibodies in an atherosclerotic rabbit model, both of which showed limited resolution.[29,30] Therefore, the development of MT1-MMP specific probes could offer distinctive physiological information *in vivo*, which EC-MMP targeted probes cannot provide.

In this study, we report a new *in vivo* method for rapid, efficient visualization of MT-MMP activity. From the known core substrate of MT1-MMP, we synthesized a new type of MT-MMP-targeted fluorogenic probe and characterized its physicochemical properties *in vitro*. MT-MMPs specificity *in vivo* was tested in MT1-MMP-overexpressing tumor-bearing mouse models by using a small animal optical imaging instrument, and the probe's efficacy was further confirmed by *ex vivo* biodistribution and immnuohistological studies.

2. MATERIALS AND METHODS

2.1. MT1-MMP Fluorogenic Probe (MT-P). A synthetic scheme is described in the Supporting Information (Scheme S1). Intermediate compound **3** Gly-Arg(Pbf)-Ile-Gly-Phe-Leu-Arg(Pbf)-Thr-Ala-Lys(Boc)-Gly-Gly was synthesized on an automatic peptide synthesizer (C S Bio Co., Menlo Park, CA) by fluorenylmethoxycarbonyl (Fmoc) chemistry at a 0.1 mmol scale using a Gly-2-ClTrt resin (0.43 meq/g). *O*-Benzotriazole-*N*,*N*,*N*′,*N*′-tetramethyl-uronium-hexafluoro-phosphate (HBTU) and hydroxybenotriazole (HOBt) were used as the activating reagents. Crude peptide was cleaved from the resin by 1% trifluoroacetic acid (TFA) in dichloromethane, followed by precipitation in cold ethyl ether. Crude peptide was purified by preparative reversed-phase high performance liquid chromatography (RP-HPLC, Dionex, Sunnyvale, CA), using 20% to 90% acetonitrile containing 0.1% TFA versus distilled water containing 0.1% TFA over 30 min at a flow rate of 10 mL/min. The proper fraction was collected and lyophilized. Then the fluorescence donor, Cy5.5 mono-*N*-hydroxysuccinamide ester (Cy5.5-NHS, 10 μM), was reacted with **3** in anhydrous dimethylformamide (200 μL) containing 2% diisopropylethylamine (DIPEA) at room temperature in the dark. The reaction was monitored by analytical RP-HPLC. Crude product **4** was precipitated by the addition of cold ethyl ether and then lyophilized. The side chain protecting groups were then removed by a TFA/water/triisopropylsilane/1,2-ethanedithiol (92.5:2.5:2.5:2.5, v/v/v/v) cleavage cocktail. **5** was purified by preparative RP-HPLC (C18 column, 5 μm, 250 × 20 mm) and lyophilized as described above. Finally, the NHS ester of Black Hole Quencher 3 (BHQ-3-NHS) was coupled to the ε-amino group of lysine, and **6**, MT-P, was purified and lyophilized. The purity was confirmed by analytical RP-HPLC (C18 column, 5 μm, 250 × 4.6 mm), and the molecular weight was confirmed by LC/MS (Figure 1).

2.2. Enzyme Specificity. The fluorogenic property of MT-P was examined by incubating 50 nM of MT-P in reaction buffer (50 mM Tris, 10 mM $CaCl_2$, 150 mM NaCl, 0.05% Brij35, pH 7.8) containing, variously, 40 nM of activated MMP-2, MMP-9 (R&D Systems Inc., Minneapolis, MN), MT1-MMP (MMP-14), MT2-MMP (MMP-15), or MT3-MMP (MMP-16). MT-MMPs were constructed and purified as described previously.[23] Inactive MMPs were activated by incubation with 2.5 mM of *p*-aminophenyl mercuric acid (APMA) in the reaction buffer for 2 h at 37 °C. After incubation in the reaction buffer at 37 °C for 60 min with respective MMPs, the NIR fluorescence emission signals of the samples were measured using a spectrofluorometer (F-7000 fluorescence spectrophotometer, Hitach, Tokyo, Japan). The excitation wavelength was set at 675 nm, and the emission spectrum was recorded from 680 to 800 nm.

2.3. Cell Culture and Animal Models. MDA-MB-435 cancer cells acquired from American Type Culture Collection (Rockville, MD) was cultured under standard culture conditions in L-15 medium containing 10% (v/v) fetal bovine serum (Invitrogen, Carlsbad, CA) supplemented with penicillin (100 μg/mL) and streptomycin (100 μg/mL). All animal studies were conducted in accordance with the principles and procedures outlined in the National Institutes of Health Guide for the Care and Use of Animals and under protocols approved by the NIH Clinical Center Animal Care and Use Committee (CC/ACUC). For the MDA-MB-435 tumor model, tumor cells (5×10^6) were subcutaneously injected into the right shoulder of female athymic nude mice (5−6 weeks old, Harlan Laboratories, Frederick, MD) at a volume of 80 μL. The mice were used for optical imaging studies when the tumor volume reached 100−300 mm^3.

2.4. Western Blot Analysis. The expression of MT1-MMP in MDA-MB-435 cells was analyzed by Western blot analysis with an MT1-MMP antibody.[23] The cell lysates were prepared in radioimmunoprecipitation assay (RIPA) buffer (Sigma), and the concentration of the whole cell protein was determined by the Bradford method. Cell proteins were subjected to 10% sodium dodecyl sulfate−polyacrylamide gel electrophoresis (SDS-PAGE), and 20 μL samples were loaded in each lane. Proteins separated in the gel were transferred to a nitrocellulose membrane by wet blotting at 300 mA for 2 h and subsequently treated with 0.5% bovine serum albumin (BSA) in Tris-buffered saline (TBS) to saturate nonspecific protein-binding sites. The membranes were then incubated with rabbit anti-MT1-MMP primary antibody (1:5000, Abcam Inc., Cambridge, MA) at a concentration of 10 μg/mL at 4 °C overnight. The membranes were washed, and protein was detected by an horseradish peroxidase (HRP)-conjugated donkey antirabbit secondary antibody. The bands on the blot were developed using an electrochemiluminescence (ECL) kit at room temperature.

2.5. *In Vivo* Imaging and *Ex Vivo* Biodistribution. *In vivo* imaging was performed and analyzed using a Maestro 2.10 *in vivo* imaging system (Cambridge Research & Instrumentation, Woburn, MA; excitation = 675 nm, emission = 695 nm). MT-P (100 μL in PBS, 5 nmol) was injected intravenously into MDA-MB-435 tumor-bearing mice via a tail vein, and imaging was performed at 1, 2, 3, 4, and 24 h after the injection of the probe (n = 3/group). During the injection and image acquisition process, the mice were anesthetized with 2.5% isoflurane in oxygen delivered at a flow rate of 1.5 L/min. To inhibit MMP expression, 1 μmol of a broad spectrum MMP inhibitor (MMPI IV, EMD Chemicals Inc., Gibbstown, NJ) was injected intratumorally 30 min prior to injection of MT-P. All images were normalized and analyzed using Maestro software. For quantitative comparison, regions of interest (ROI) were drawn over tumors and muscle, and the average signal (10^6 photons × cm^{-2} × s^{-1}) for each area was measured.

For the *ex vivo* biodistribution study, mice were sacrificed 24 h postinjection, and tumor tissues and major organs were carefully harvested. All samples were rinsed with saline, placed on black paper, and immediately imaged using Maestro. For quantitative comparison, ROIs were calculated as described above.

2.6. Immunohistology. MDA-MB-435 tumors from the tumor-bearing mice were frozen in optimal cutting temperature (OCT) embedding medium. Cryosections were cut into 4 μm slices and stained. Briefly, tumor slides were dried in the air and fixed with cold acetone for 20 min and dried again in air for 30 min at room temperature. After blocking with 10% BSA for 30 min, the sections were incubated with rabbit anti-MT1-MMP

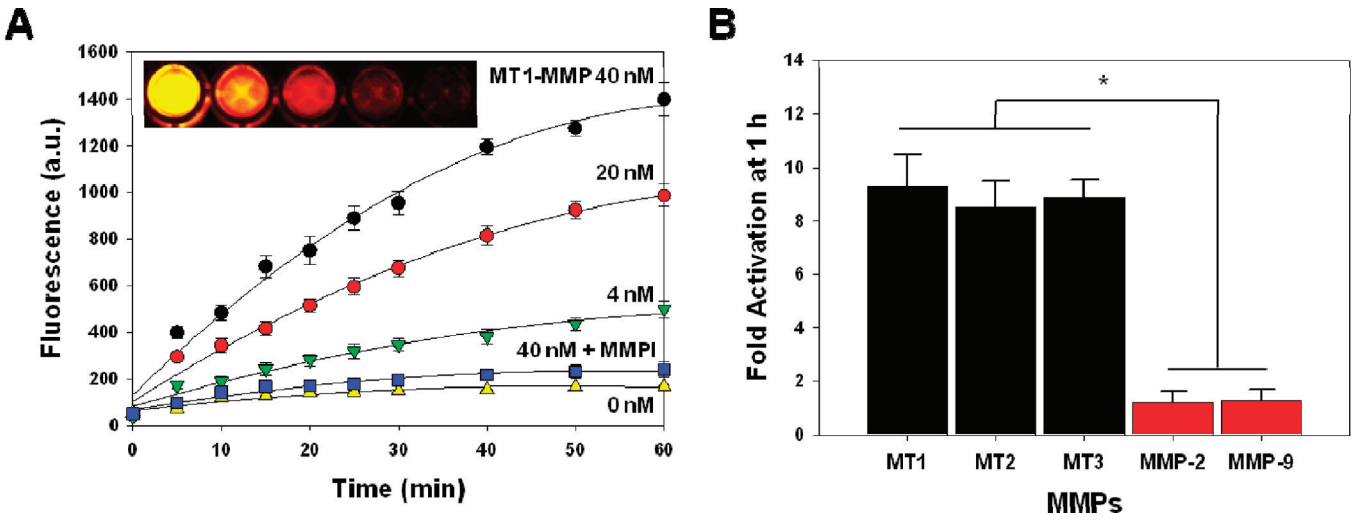

Figure 2. Recovery of fluorescence of MT-P in the presence of various activated MMPs. (A) Fluorescence emission kinetic spectra of MT-P in the presence of various concentrations of activated MT1-MMP (0, 4, 20, and 40 nM) and MT1-MMP (40 nM) with a broad spectrum MMP inhibitor (MMP-I) following a 60 min incubation at 37 °C. (B) Fluorescence activation of MT-P in a solution containing various activated MMPs following a 60 min incubation at 37 °C. Means ± SD (n = 3). *P < 0.05 for MT-MMPs relative to EC-MMPs.

antibody (10 μg/mL) for 60 min at room temperature in the dark and then visualized with fluorescein isothiocyanate (FITC)-conjugated donkey antirabbit secondary antibody. Finally, the slices were mounted with 4′,6-diamidino-2-phenylindole (DAPI)-containing mounting medium under an epifluorescence microscope (Olympus, X81). For NIR fluorescence imaging, tumor sections were imaged by a fluorescence microscope equipped with a Cy5.5 filter setting.

2.7. Statistical Analysis. Quantitative data were expressed as mean ± SD (standard deviation). Two-tailed paired and unpaired Student's t tests were used to test differences within groups and between groups, respectively. P values of less than 0.05 were considered statistically significant.

3. RESULTS AND DISCUSSION

3.1. Design of MT1-MMP-Specific Fluorogenic Probe. As described in Figure 1, the MT-MMP fluorogenic probe MT-P is composed of NIR dye (Cy5.5), MT-MMP substrate, and BHQ-3 (as the NIR dark-quencher). The MT1-MMP cleavable substrate, Gly-*Arg-Ile-Gly-Phe-Leu-Arg*-Thr-Ala-Lys-Gly-Gly, was synthesized by standard solid-phase Fmoc peptide chemistry. The recognition site is indicated by italics, and the cleavage site is between Phe and Leu. Since all of the MMPs share a high degree of domain structural homology, it is important to use a highly selective substrate for a target MMP in probe design. Optimal peptide substrates for specific MMP can be identified using a substrate phage display technique. The core substrate of MT1-MMP, Arg-Ile-Gly-Phe-Leu-Arg, was adopted from a previous report. Kridel et al. reported several peptides, selected from a phage display peptide library, with high MT1-MMP specificity, and we chose the substrate with the highest specificity and selectivity for MT1-MMP.[31] This substrate was reported as highly selective for MT1-MMP, among the commonly studied extracellular MMPs associated with tumor generation and development, such as MMP-2 and MMP-9 (with specificity constants (k_{cat}/K_m) for MT1-MMP and MMP-9 of 777 200 and 20 000 M^{-1} s^{-1}, respectively).[31] Amino acids including Gly and Lys were incorporated in a core substrate as residues for dye conjugation and as spacers between substrate and dye molecules. MT-P showed a purity greater than 95% by RP-HPLC and UV−vis spectra with two absorption maxima at 630 and 685 nm in PBS for BHQ-3 and Cy5.5, respectively (Figure 1B). The mass was confirmed by LC/MS (m/z calculated, 2662.13; found, $[M + 2H]^{2+}$) (Figure 1C).

3.2. *In Vitro* Studies: MT1-MMP Specificity. The NIR fluorescent signal amplification of MT-P against MT1-MMP was evaluated *in vitro* by incubating MT-P with different concentrations of MT1-MMP (0, 4, 20, and 40 nM) with and without a broad spectrum MMP inhibitor in the reaction buffer. NIR fluorescence emission signals of MT-P were measured by spectrofluorometer for 60 min. As shown in Figure 2A, MT-P demonstrated a proportional relationship between recovered NIR fluorescent signals and MT1-MMP concentrations. The spectrofluorimetry plots clearly indicate that MT1-MMP was able to activate NIR fluorescent signals of MT-P up to 10-fold over the probe without MT1-MMP. The activation of MT-P was inhibited in the presence of an inhibitor MMP-I, suggesting evidence for the selectivity of the probe. The activation process was simply visualized by NIR fluorescence after each sample was transferred to a 96-well microplate and subjected to Maestro 2 imaging (Figure 2A). MT1-MMP selectivity was measured under the same experimental setup with different MMPs including MT1, MT2, MT3-MMPs (MMP-14, 15, 16), MMP-2, and MMP-9. The pro form of both MMP-2 and MMP-9 were activated by *p*-aminophenyl mercuric acid (APMA) in the reaction buffer before use as previously described.[21] As shown in Figure 2B, MT-P demonstrated significantly higher activation folds when incubated with MT-MMPs than with extracellular MMPs (activation folds for MT1, 2, 3-MMP, and MMP-2,-9 were 9.3 ± 1.2, 8.5 ± 0.9, 8.9 ± 0.6, 1.2 ± 0.4, and 1.3 ± 0.4, respectively). The recognition of MT1-MMP substrate by different MT-MMPs, such as MT2- and MT3-MMP, was not previously reported,[31] and this may be related to the sharing of similar catalytic domains among the MT-MMPs. Since MT-P was shown to be recognized and activated significantly by different MT-MMPs, but not by extracellular MMPs such as MMP-2 and -9, it can be used as an MT-MMP specific probe.

3.3. *In Vivo* Studies: Imaging of MT1-MMP Expression in Tumor-Bearing Mice. After validation of MT-P's utility *in vitro*, the potential for its *in vivo* application was investigated using tumor-bearing mice models and a small animal optical imaging system, Maestro 2. Before performing *in vivo* imaging, we evaluated the overexpression of MT1-MMP in MDA-MB-435 cells and in xenografted tumors by Western blot and immunohistochemistry, respectively. MT1-MMP (64 kDa) was strongly expressed in MDA-MB-435 cells (Figure 3A). As expected, MT1-MMP was also highly expressed in MDA-MB-435 tumor sections, verified by fluorescent immunostaining using a MT1-MMP antibody (Figure 3B–D).

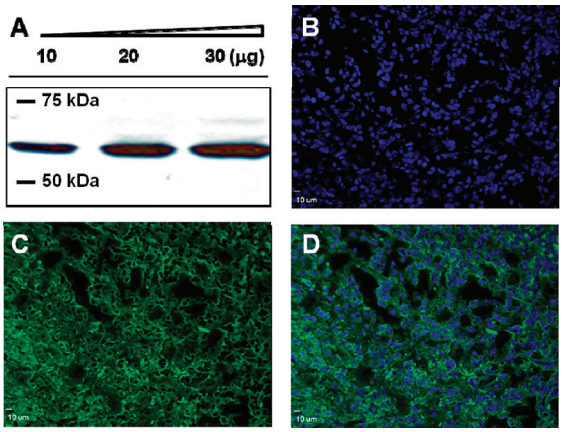

Figure 3. (A) Representative Western blot analyses of MDA-MB-435 cell lysates for MT1-MMP (64 kDa). (B–D) Fluorescent immunostaining of MT1-MMP expression in an MDA-MB-435 tumor section counterstained with (B) DAPI (blue, marks the nucleus), (C) primary antibody for MT1-MMP, and (D) their merged images.

To evaluate whether MT-P can image the MT1-MMP activities *in vivo*, MT-P was administered intravenously into MT1-MMP-positive MDA-MB-435-tumor-bearing mice. *In vivo* imaging was performed over 24 h. Figure 4A shows representative *in vivo* whole-body images of animals at selected time points (1, 2, 3, 4, and 24 h) after injection. MT-P demonstrated strong NIR fluorescent activations in the MT1-MMP-positive tumor region. It should be noted that the probe clearly showed early onset of activation (in less than 1 h) and the high fluorescent signals in the tumor were maintained up to 24 h. When a MMP-I was injected intratumorally 30 min before the probe injection to inhibit the MT1-MMP activity, the NIR fluorescent signals were significantly reduced (Figure 4A). MMP-I is a broad spectrum, hydroxamate-based MMP inhibitor and known to inhibit MMPs including MMP-2 and MMP-9.[32] Their inhibition specificities against MT-MMPs were not reported; based on our experimental results (Figure 2A), MMP-I inhibited MT-MMP activity as like other hydroxamate-based MMP inhibitor reported previously.[33] The ratio of the signal in the ROI of the tumor compared to the muscle region (T/M ratio) revealed that fluorescent signals gradually increased up to 4 h after the probe injection and could accumulate and remain sustained (Figure 4B) for 24 h. In contrast, the activation of MT-P was suppressed at all time points when the activity of MT1-MMP was restrained by the MMP inhibitor (T/M ratio of MT-P without and with the MMP inhibitor at 24 h postinjection, 3.0 ± 0.2 and 1.2 ± 0.1, respectively).

3.4. *Ex Vivo* Studies: Biodistribution and Histology. *Ex vivo* imaging of excised tumors and other organs was also performed after 24 h of *in vivo* imaging to confirm the specific activation of MT-P in tumors. As shown in Figure 5A–C, biodistribution studies indicated that MT-P without an inhibitor activated predominantly in the tumor and liver over other organs. These were unexpected results, because strong activation of fluorogenic probe in the liver was not observed in our previous report.[20,21] When animals are placed in a prone position for whole body imaging, the fluorescent signals from the liver can be undervalued due to the depth resolution limit in optical imaging. In our previous report, where the biodistribution studies were performed at 4 h postinjection, all of the fluorogenic probes designed for extracellular MMPs showed at least 2 to 5-fold higher fluorescent intensity in the tumor

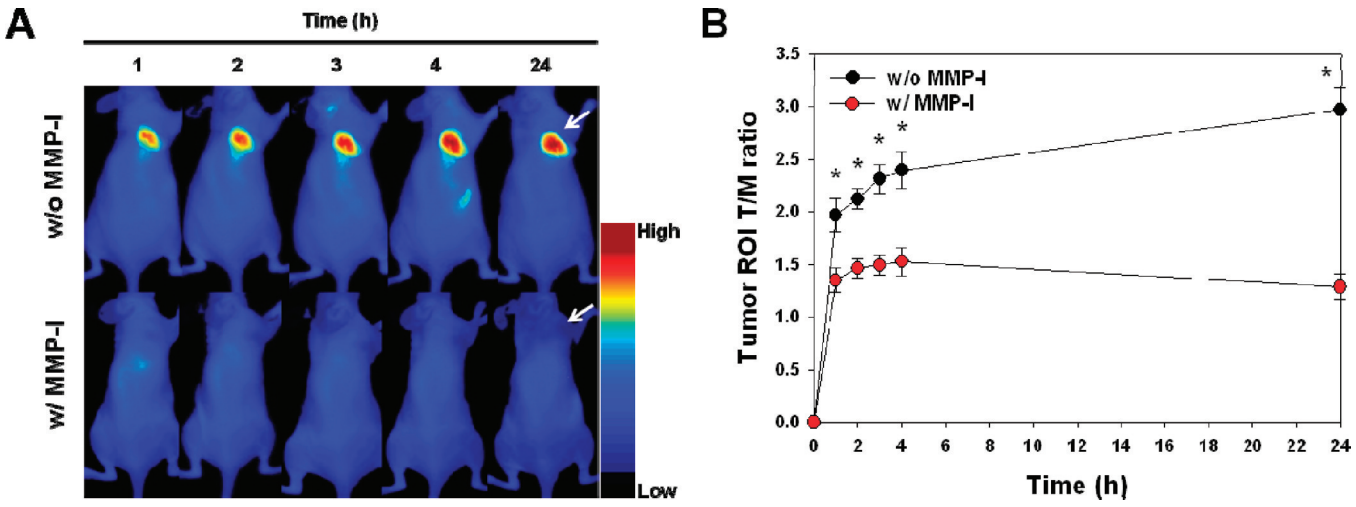

Figure 4. Whole-mouse optical imaging. (A) Representative serial *in vivo* NIR fluorescence images of MT1-MMP-positive MDA-MB-435 tumor-bearing mice injected intravenously with MT-P under conditions without and with MMP inhibitor (MMP-I). Images were acquired at the indicated time points and were normalized by the maximum average value. The color bar indicates radiant efficiency (low, 0; high, 0.139×10^6). Arrows indicate tumors. (B) Tumor ROI T/M ratio (the ratio of the signal in the ROI of the tumor compared to the muscle region) analysis of MDA-MB-435 tumor *in vivo*. Means ± SD (n = 3–6 per group). *P < 0.05.

dx.doi.org/10.1021/mp2002297 | *Mol. Pharmaceutics* 2011, 8, 2331–2338

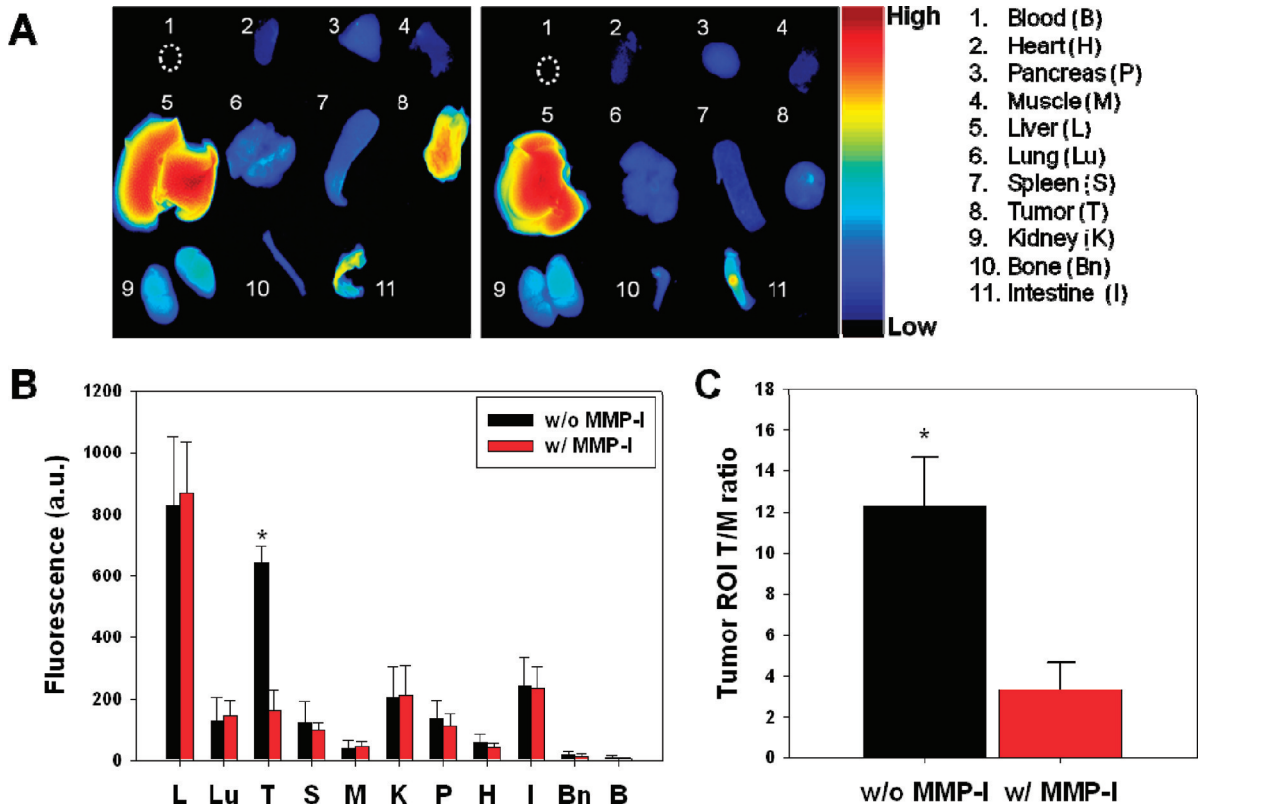

Figure 5. (A) Representative images of dissected organs and tissues of MDA-MB-435 tumor-bearing mice sacrificed at 24 h after intravenous injection of MT-P without (left) and with (right) MMP-I. The color bar indicates radiant efficiency (low, 0; high, 0.133×10^6). (B) Biodistribution of MT-P at 24 h postinjection. (C) Tumor ROI T/M analysis of fluorescence intensity in excised tumor. Means ± SD (n = 3–6 per group). *P < 0.05.

compared to the liver signal. Strong signals from the liver might be a result of specific proteolytic degradations of MT-P by certain proteases in the liver, and/or the probe is structurally suited to localize in the liver and nonspecifically degrade. Even though MT-P showed nonspecific activation in the liver, the probe clearly demonstrated *in vivo* imaging of MT1-MMP activity; a fluorescence microscope showed strong fluorescence signals in tumor sections (taken from areas that fluoresced during *in vivo* imaging), when the sections were injected with MT-P, but not when the sections were simultaneously injected with an MMP-I (Figure 6).

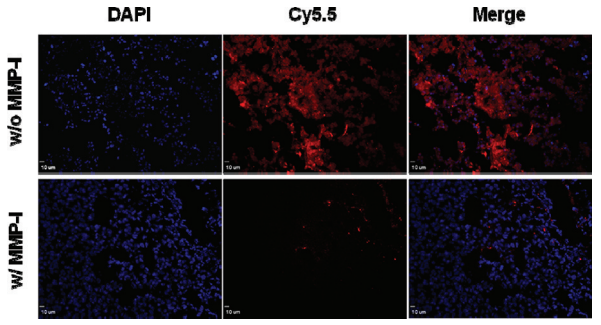

Figure 6. NIR fluorescence images of tumor sections injected with MT-P (red) without and with MMP-I. Tumor sections were counterstained with DAPI (blue). Scale bar, 10 μm.

We initially thought that MT-P would provide only marginal NIR fluorescent signals in tumors *in vivo* because (i) MT1-MMP is tethered to the cellular membrane, which requires the probe be activated on the tumor cell membrane and, thus, with a lower accessibility than the soluble type of extracellular MMPs, which is freely available around the tumor cells, and (ii) the probe is simply comprised of peptide substrate and dyes without any further modification. A solely peptide-based fluorogenic probe, without modification with polymers and/or nanomaterials, typically has limited applications due to modest fluorescent changes *in vivo* with low T/M ratios, due to poor physicochemical properties such as stability and solubility and unfavorable pharmacokinetics. However, as our results demonstrated, a simple form of fluorogenic peptide is recognized and activated by a target protease expressed on the cellular membrane *in vivo*. More importantly, an activated probe enabled apparent visualization of MT1-MMP activity in the tumor region in less than one hour, and the strong signals were maintained for up to 24 h. It has been reported that an amphiphilic dye, such as Cy5.5, can remain localized in the tissues instead of being washed away by the blood once it is activated in the tumor region.[20] Interestingly, Cy5.5 released from MT-P accumulated within the tumor over a longer time (~24 h) compared to a fluorogenic probe activated by extracellular MMPs (~ 12 h). The fluorescent signal in the tumor was not detectable at 48 h postinjection. It is possible that the amphiphilic Cy5.5 dye, when activated by membrane-bound MMPs in tumor cells, diffuses more efficiently through the plasma membrane than a dye activated by MMPs around the tumor cells. This may explain why a small peptide-based fluorogenic probe shows clear and bright fluorescent signals and allows rapid identification of *in vivo* MT1-MMP activity in tumors. Although MT-P showed good specificity in an MT1-

MMP-positive tumor, its nonspecific activation and accumulation in the liver not only diminishes the future utilities of the probe but also can result in possible liver toxicity. Therefore, the probe should be optimized and screened further for improved *in vivo* specificity and selectivity followed by careful metabolic and toxicity studies of MT-P in the liver. In addition, the correlation between fluorescent signal intensities and tumor volume should be verified *in vivo*.

4. CONCLUSIONS

In this report, we describe the design of an MT-MMP-specific probe and demonstrate for the first time the possibility of using a fluorogenic probe to monitor expression and inhibition of MT-MMPs *in vivo*. The probe is able to recover strong fluorescent signals against different types of MT-MMPs, but not against EC-MMPs such as MMP-2 and MMP-9. Importantly, we show that a fluorogenic probe can be activated rapidly and efficiently by membrane-tethered proteases *in vivo*, just as by soluble-type extracellular proteases. In addition, fluorogenic probes targeting MT-MMPs retain prolonged and strong fluorescent signals in tumors when compared to similar probes targeting EC-MMPs. We expect that any of the reported membrane-tethered protease substrate can be incorporated successfully into a fluorogenic probe constructed to serve as an imaging agent, such as the one reported here, to visualize and monitor protease activities on plasma membranes. Our findings offer the design of new types of membrane-bound protease targeting probes that have the potential to improve understanding of the roles of membrane-associated proteases and the capability to screen *in vivo* for more specific protease inhibitors.

■ ASSOCIATED CONTENT

Ⓢ Supporting Information

Details of synthesis methods (Scheme S1). This material is available free of charge via the Internet at http://pubs.acs.org.

■ AUTHOR INFORMATION

Corresponding Author

*Mailing address: 31 Center Dr. 1C22, Bethesda, MD 20892, United States. Phone: 301-451-4246; fax: 301-480-0679; e-mail: shawn.chen@nih.gov and seulki.lee@nih.gov.

■ ACKNOWLEDGMENTS

This work was supported in part by the Intramural Research Program (IRP), National Institute of Biomedical Imaging and Bioengineering (NIBIB), National Institutes of Health (NIH), and the International Cooperative Program of the National Science Foundation of China (NSFC) (81028009). L.Z. is partially supported by the Chinese Scholarship Council (CSC). S.L. is partially supported by the NIH pathway to independence (K99/R00) award. We thank Ms. Maggie Swierczewska and Dr. Henry S. Eden for proof-reading the manuscript.

■ REFERENCES

(1) Liotta, L. A.; Tryggvason, K.; Garbisa, S.; Hart, I.; Foltz, C. M.; Shafie, S. Metastatic potential correlates with enzymatic degradation of basement membrane collagen. *Nature* **1980**, *284* (5751), 67–8.

(2) Egeblad, M.; Werb, Z. New functions for the matrix metalloproteinases in cancer progression. *Nat. Rev. Cancer* **2002**, *2* (3), 161–74.

(3) Kessenbrock, K.; Plaks, V.; Werb, Z. Matrix metalloproteinases: regulators of the tumor microenvironment. *Cell* **2010**, *141* (1), 52–67.

(4) Coussens, L. M.; Fingleton, B.; Matrisian, L. M. Matrix metalloproteinase inhibitors and cancer: trials and tribulations. *Science* **2002**, *295* (5564), 2387–92.

(5) Lee, M.; Fridman, R.; Mobashery, S. Extracellular proteases as targets for treatment of cancer metastases. *Chem. Soc. Rev.* **2004**, *33* (7), 401–9.

(6) Turk, B. Targeting proteases: successes, failures and future prospects. *Nat. Rev. Drug Discovery* **2006**, *5* (9), 785–99.

(7) Lee, S.; Xie, J.; Chen, X. Activatable molecular probes for cancer imaging. *Curr. Top. Med. Chem.* **2010**, *10* (11), 1135–44.

(8) Scherer, R. L.; McIntyre, J. O.; Matrisian, L. M. Imaging matrix metalloproteinases in cancer. *Cancer Metastasis Rev.* **2008**, *27* (4), 679–90.

(9) Overall, C. M.; Kleifeld, O. Tumour microenvironment - opinion: validating matrix metalloproteinases as drug targets and anti-targets for cancer therapy. *Nat. Rev. Cancer* **2006**, *6* (3), 227–39.

(10) Roy, R.; Yang, J.; Moses, M. A. Matrix metalloproteinases as novel biomarkers and potential therapeutic targets in human cancer. *J. Clin. Oncol.* **2009**, *27* (31), 5287–97.

(11) Olson, E. S.; Jiang, T.; Aguilera, T. A.; Nguyen, Q. T.; Ellies, L. G.; Scadeng, M.; Tsien, R. Y. Activatable cell penetrating peptides linked to nanoparticles as dual probes for *in vivo* fluorescence and MR imaging of proteases. *Proc. Natl. Acad. Sci. U.S.A.* **2010**, *107* (9), 4311–6.

(12) Lee, S.; Park, K.; Lee, S. Y.; Ryu, J. H.; Park, J. W.; Ahn, H. J.; Kwon, I. C.; Youn, I. C.; Kim, K.; Choi, K. Dark quenched matrix metalloproteinase fluorogenic probe for imaging osteoarthritis development *in vivo*. *Bioconjugate Chem.* **2008**, *19* (9), 1743–7.

(13) Zheng, G.; Chen, J.; Stefflova, K.; Jarvi, M.; Li, H.; Wilson, B. C. Photodynamic molecular beacon as an activatable photosensitizer based on protease-controlled singlet oxygen quenching and activation. *Proc. Natl. Acad. Sci. U.S.A.* **2007**, *104* (21), 8989–94.

(14) Wagner, S.; Breyholz, H. J.; Law, M. P.; Faust, A.; Holtke, C.; Schroer, S.; Haufe, G.; Levkau, B.; Schober, O.; Schafers, M.; Kopka, K. Novel fluorinated derivatives of the broad-spectrum MMP inhibitors N-hydroxy-2(R)-[[(4-methoxyphenyl)sulfonyl](benzyl)- and (3-picolyl)-amino]-3-methyl-butanamide as potential tools for the molecular imaging of activated MMPs with PET. *J. Med. Chem.* **2007**, *50* (23), 5752–64.

(15) Bazeli, R.; Coutard, M.; Duport, B. D.; Lancelot, E.; Corot, C.; Laissy, J. P.; Letourneur, D.; Michel, J. B.; Serfaty, J. M. *In vivo* evaluation of a new magnetic resonance imaging contrast agent (P947) to target matrix metalloproteinases in expanding experimental abdominal aortic aneurysms. *Invest. Radiol.* **2010**, *45* (10), 662–8.

(16) Lee, S.; Park, K.; Kim, K.; Choi, K.; Kwon, I. C. Activatable imaging probes with amplified fluorescent signals. *Chem. Commun. (Cambridge)* **2008**, *36*, 4250–60.

(17) Lee, S.; Xie, J.; Chen, X. Peptides and peptide hormones for molecular imaging and disease diagnosis. *Chem. Rev.* **2010**, *110* (5), 3087–111.

(18) Bremer, C.; Tung, C. H.; Weissleder, R. *In vivo* molecular target assessment of matrix metalloproteinase inhibition. *Nat. Med.* **2001**, *7* (6), 743–8.

(19) Aguilera, T. A.; Olson, E. S.; Timmers, M. M.; Jiang, T.; Tsien, R. Y. Systemic *in vivo* distribution of activatable cell penetrating peptides is superior to that of cell penetrating peptides. *Integr. Biol. (Cambridge)* **2009**, *1* (5–6), 371–81.

(20) Zhu, L.; Xie, J.; Swierczewska, M.; Zhang, F.; Quan, Q.; Ma, Y.; Fang, X.; Kim, K.; Lee, S.; Chen, X. Real-Time Video Imaging of Protease Expression *In vivo*. *Theranostics* **2011**, *1*, 18–27.

(21) Lee, S.; Ryu, J. H.; Park, K.; Lee, A.; Lee, S. Y.; Youn, I. C.; Ahn, C. H.; Yoon, S. M.; Myung, S. J.; Moon, D. H.; Chen, X.; Choi, K.; Kwon, I. C.; Kim, K. Polymeric nanoparticle-based activatable near-infrared nanosensor for protease determination *in vivo*. *Nano Lett.* **2009**, *9* (12), 4412–6.

(22) McIntyre, J. O.; Fingleton, B.; Wells, K. S.; Piston, D. W.; Lynch, C. C.; Gautam, S.; Matrisian, L. M. Development of a novel fluorogenic proteolytic beacon for *in vivo* detection and imaging of

tumour-associated matrix metalloproteinase-7 activity. *Biochem. J.* **2004**, *377* (Pt 3), 617−28.
(23) Zhu, L.; Wang, H.; Wang:..; Wang, Y.; Jiang, K.; Li, C.; Ma, Q.; Wang, L.; Li, W.; Cai, M.; Wang, H.; Niu, G.; Lee, S.; Yang, W.; Fang, W.; Chen, X. High-affinity peptide against MT1-MMP for *in vivo* tumor imaging. *J. Controlled Release* **2011**, *150* (3), 248−55.
(24) Sato, H.; Takino, T.; Okada, Y.; Cao, J.; Shinagawa, A.; Yamamoto, E.; Seiki, M. A matrix metalloproteinase expressed on the surface of invasive tumour cells. *Nature* **1994**, *370* (6484), 61−5.
(25) Seiki, M. Membrane-type 1 matrix metalloproteinase: a key enzyme for tumor invasion. *Cancer Lett.* **2003**, *194* (1), 1−11.
(26) Arroyo, A. G.; Genis, L.; Gonzalo, P.; Matias-Roman, S.; Pollan, A.; Galvez, B. G. Matrix metalloproteinases: new routes to the use of MT1-MMP as a therapeutic target in angiogenesis-related disease. *Curr. Pharm. Des.* **2007**, *13* (17), 1787−802.
(27) Moss, N. M.; Barbolina, M. V.; Liu, Y.; Sun, L.; Munshi, H. G.; Stack, M. S. Ovarian cancer cell detachment and multicellular aggregate formation are regulated by membrane type 1 matrix metalloproteinase: a potential role in I.p. metastatic dissemination. *Cancer Res.* **2009**, *69* (17), 7121−9.
(28) Ueda, J.; Kajita, M.; Suenaga, N.; Fujii, K.; Seiki, M. Sequence-specific silencing of MT1-MMP expression suppresses tumor cell migration and invasion: importance of MT1-MMP as a therapeutic target for invasive tumors. *Oncogene* **2003**, *22* (54), 8716−22.
(29) Van Steenkiste, M.; Oltenfreiter, R.; Frankenne, F.; Vervoort, L.; Maquoi, E.; Noel, A.; Foidart, J. M.; Van De Wiele, C.; De Vos, F. Membrane type 1 matrix metalloproteinase detection in tumors, using the iodinated endogenous [^{123}I]-tissue inhibitor 2 of metalloproteinases as imaging agent. *Cancer Biother. Radiopharm.* **2010**, *25* (5), 511−20.
(30) Kuge, Y.; Takai, N.; Ogawa, Y.; Temma, T.; Zhao, Y.; Nishigori, K.; Ishino, S.; Kamihashi, J.; Kiyono, Y.; Shiomi, M.; Saji, H. Imaging with radiolabelled anti-membrane type 1 matrix metalloproteinase (MT1-MMP) antibody: potentials for characterizing atherosclerotic plaques. *Eur. J. Nucl. Med. Mol. Imaging* **2010**, *37* (11), 2093−104.
(31) Kridel, S. J.; Sawai, H.; Ratnikov, B. I.; Chen, E. I.; Li, W.; Godzik, A.; Strongin, A. Y.; Smith, J. W. A unique substrate binding mode discriminates membrane type-1 matrix metalloproteinase from other matrix metalloproteinases. *J. Biol. Chem.* **2002**, *277* (26), 23788−93.
(32) Zhu, L.; Xie, J.; Swierczewska, M.; Zhang, F.; Lin, X.; Fang, X.; Niu, G.; Lee, S.; Chen, X. Dual-functional, receptor-targeted fluorogenic probe for *in vivo* imaging of extracellular protease expressions. *Bioconjugate Chem.* **2011**, *22* (6), 1001−5.
(33) Butler, G. S.; Dean, R. A.; Tam, E. M.; Overall, C. M. Pharmacoproteomics of a metalloproteinase hydroxamate inhibitor in breast cancer cells: dynamics of membrane type 1 matrix metalloproteinase-mediated membrane protein shedding. *Mol. Cell. Biol.* **2008**, *28* (14), 4896−914.